Possible Bose-Einstein condensate associated with an orbital degree of freedom in the Mott insulator CaCrO_{3}

J.-S. Zhou, L.-P. Cao, J. A. Alonso, J. Sanchez-Benitez, M. T. Fernandez-Diaz, X. Li, J.-G. Cheng, L. G. Marshall, C.-Q. Jin, and J. B. Goodenough

Phys. Rev. B **94**, 155137 — Published 21 October 2016

DOI: 10.1103/PhysRevB.94.155137

A possible Bose-Einstein condensate associated with an orbital degree of freedom in the Mott insulator $CaCrO_3$

J.-S. Zhou[1]*, L.-P. Cao[2], J.A. Alonso[3], J. Sanchez-Benitez[4], M.T. Fernandez Diaz[5], X. Li[1,2], J.-G. Cheng[2], L. Marshall[1], C.-Q. Jin[2], J.B. Goodenough[1],

[1] Materials Science and Engineering program/Mechanical Engineering, University of Texas at Austin, USA
[2] Institute of Physics, Chinese Academy of Sciences, Beijing 100190, China
[3] Instituto de Ciencia de Materiales de Madrid, CSIC, Cantoblanco, E-28094 Madrid, Spain
[4] Departamento de Quimica Fisica, Fac.CC. Quimicas, Universidad Complutense de Madrid, E-28040 Madrid, Spain
[5] Institute Laue-Langevin (ILL) 156X, F-38042 Grenoble Cedex 9, France

Whether $CaCrO_3$ is a Mott insulator or a correlated metal is still controversial. We have performed measurements of magnetization, specific heat, and thermal conductivity on $CaCrO_3$ samples selected from many batches of high-pressure synthesis. The single crystal $CaCrO_3$ sample exhibits an unprecedentedly sharp transition at a Néel temperature $T_N \approx 90$ K. The critical behavior of specific heat cannot be rationalized by the renormalization group theory for a second order magnetic transition. More surprisingly, the thermal conductivity κ exhibits an anomalous drop on cooling through T_N, which is opposite to all known influence on κ from either spin or orbital ordering. We have argued, on the basis of anomalies found in all three measurements and structural data, for the coexistence of itinerant π-bonding electrons in a *c*-axis band and localized xy electrons in xy orbitals responsible for type-C antiferromagnetic order below T_N and the occupation of a pure, localized xy orbital undergoing a Bose Einstein condensate (BEC) at T_N.

The perovskite $CaCrO_3$ has drawn considerable attention in recent years.[1-8] The available experimental results of this perovskite are still controversial. An early-day study on a crystal grain showed a metallic conduction to the lowest temperature with a small jump of resistivity on cooling through T_N.[9] For polycrystalline samples, a high and activated resistivity was found.[5] However, an optical study on polycrystalline samples showed a finite conductivity at $\omega = 0$, which is evidence for a metal.[4,5,7] On the other hand, neutron diffraction on a $CaCrO_3$ sample has revealed an evolution of a local structural change as a function of temperature and a type-C antiferromagnetic ordering below $T_N \approx 90$ K.[4,5] The finding of a collinear type-C antiferromagnetic ordering, typical for localized electrons, contradicts the conclusion of itinerant electrons from the reflectivity measurement. The local structural distortion also reflects an unusual electronic state and unprecedented orbital dynamics. The orthorhombic *Pbnm* perovskite has intrinsic distortions that can be extracted from isostructural $CaTiO_3$ and $CaVO_3$ where orbital ordering is not an issue.[10,11] The intrinsic distortions bias the orbital ordering in orbitally degenerate systems such as in the t_2 electronic systems of $RTiO_3$ (R=rare earth, and Y).[12, 13, 14] Neutron diffraction[5] showed that an orbital degeneracy survives through a magnetic transition and to lower temperatures. The analysis of critical phenomena of physical properties and an unusual thermal conductivity at T_N indeed reveal new physics associated with the interaction between spins and orbital dynamics. We argue that while the orbital degeneracy is not removed, a giant number of collective orbital excitations undergo a Bose-Einstein condensate on cooling through the Néel temperature in $CaCrO_3$.

The $CaCrO_3$ samples were made under high pressure. Large cubes (100 ~200 μm) of $CaCrO_3$ crystal can be found in some batches of the high-pressure products. Measurements of physical properties were performed on single-crystal samples, polycrystalline samples with embedded crystal grains, and on uniformly polycrystalline samples. Detailed information about the samples' preparation, characterization and measurements of physical properties can be found in the Supplementary Information (SI).[15] Fig.1 shows the result of a magnetization measurement on a single crystal sample; the transition at T_N is remarkably sharp. In type-C ordering, the easy magnetization axis is along the ± y direction of the orthorhombic cell according to neutron diffraction studies.[4,5] For the *Pbnm* crystal structure, the compatible magnetic structure is F_xC_y of the irreducible representation Γ_2.[16] However, it is impossible for neutron diffraction to pick up a tiny spin canting in the x direction. By considering the interatomic spin-orbit coupling, Moriya

has put forward the theory of antisymmetric spin coupling in localized magnetic insulators that gives a quantitative description of spin canting and the temperature-dependent magnetization. The magnetic susceptibility for the field perpendicular to the easy axis is expressed as [17]

$$\chi = \frac{Ng^2\mu_B^2 S(S+1)}{3k(T+T_N)} \frac{T-T_0}{T-T_N} \quad , \qquad T_N = \frac{JZS(S+1)}{3k}\left[1+\left(\frac{D}{J}\right)^2\right]^{1/2} \quad , \quad T_0 = \frac{JZS(S+1)}{3k}$$

where Z is the number of nearest neighbors and D is the Dzialoshinski-Moryia coupling constant. In contrast to a regular antiferromagnet, the susceptibility for the AF system with canted spins would exhibit an extremely sharp transition at T_N. The transition area of magnetization data in Fig.1 can be fit to the expression very well; the fitting gives a D ≈ 4 K and a spin canting angle θ ≈ 0.08 ° based on tan2θ ~ D/2J from the theory. In comparison, a metallic antiferromagnet $Nb_{12}O_{29}$ shows a broad peak at T_N in the temperature dependence of magnetization.[18] It should be stressed that the antisymmetric exchange interaction has been found only in localized-electron antiferromagnets.

As shown in Fig.1, the transition at T_N in the polycrystalline samples is relatively broad. A transition at a lower temperature or multiple transitions can also be identified in the results of specific heat measurements in these samples. A lower T_N is related to oxygen non-stoichiometry in the samples.[5] Fig.2(a) shows the C_p of crystal cubes and the polycrystalline samples with/without embedded crystals. The Néel temperature T_N of these samples can be obtained from a λ-shape anomaly in the plot of C_p versus temperature. The single crystal sample exhibits the highest T_N among samples studied. As characterized by SEM in SI,[15] sample A is a uniformly polycrystalline sample, which shows a much broader transition at a relatively lower temperature. Sample B, a polycrystalline sample with a few embedded crystals, shows a slightly higher T_N than that of sample A and an anomaly at the temperature corresponding to T_N of the single crystal sample is also visible. Embedded crystals in sample C occupy more than 1/3 of the sample's volume. A λ-shape anomaly is essentially the same as that at T_N in the single crystal sample, but the magnitude is lower. All these observations demonstrate that all single- crystal grains found in different batches of high pressure synthesis have the same T_N that is higher than the broad anomaly at T_N in polycrystalline samples.

The magnetic contribution C_m to the specific heat in Fig.2(a) of single crystal $CaCrO_3$ was obtained by subtracting the lattice contribution obtained by fitting $C_p(T)$ with a combination of the Debye and Einstein formulae at temperatures away from the vicinity of T_N. The $C_m(T)$ versus the reduced temperature $t \equiv (T-T_N)/T_N$ has been compared directly with a $C_m(T)$ of typical Heisenberg magnets.[19] The transition at T_N for a single-crystal $CaCrO_3$ is significantly narrower than that for a regular second-order magnetic transition. One may be curious whether the super-sharp anomaly at T_N in $CaCrO_3$ is simply caused by a first-order transition. The structural study[5] indicated that there is no volume change. As shown in the SI,[15] a spike with extremely high magnitude and a discontinuity of C_p caused by latent heat at the first-order transition in $LuVO_3$ clearly distinguish the $C_p(T)$ found in $CaCrO_3$ from a first order transition. More importantly, a first-order transition does not come with critical fluctuations. For a second-order magnetic transition, the critical behavior can be described by a power law based on the renormalization group theory. The C_m data are well-mapped along two parallel lines in the plot of $\log C_m$ versus $\log|1-T/T_N|$ near T_N in Fig.2(b), which indicates that the critical behavior of $CaCrO_3$ can be perfectly described by a power law. However, the exponent obtained by linear fitting the plot is $\alpha^+ = -0.75(3)$, $\alpha^- = -0.75(2)$ for the data above and below T_N (= 89.089 K), which is significantly different from an $\alpha = -0.11$ for a 3D Heisenberg magnet and actually different from any exponents for a variety of magnetic models.[20] On the other hand, $C_m(T)$ of the $CaCrO_3$ crystal shares stunningly the essential feature of the C_v of ^{4}He at the λ transition from ^{4}He I to ^{4}He II.[21] The quantum liquid of ^{4}He undergoes a Bose-Einstein condensation (BEC) into the superfluid phase of ^{4}He II. In the case of the quantum spin-dimer system $Sr_3Cr_2O_8$, an extremely sharp anomaly has also been found where the applied magnetic field H is well above a critical value H_c of the quantum critical point.[22] While the spin ordering state is no different from that of a Néel state, the magnetic transition and its field dependence associated with a degenerate state for triplons can be treated by a BEC.[22,23,24] In addition to the sharp anomaly, the critical exponents for a BEC are normally different from those predicted by the renormalization group theory.[25] For example, at the λ transition of ^{4}He, a $C_v = -\alpha \ln[(T_c-T)/T_c] + b$ has been reported instead of the power law.[26] In the case of the BEC in $Sr_3Cr_2O_8$, an $\alpha \approx -0.3$ was obtained by analyzing the data in ref.22. Generally speaking, a small temperature range t_G for critical fluctuations means a longer coherence length ξ_0 based on the Ginzburg criterion $t_G = (T_G-T_c)/T_c \sim \Delta C^{-2}\xi_0^{-1}$, where ΔC is the jump of C_m at T_c or T_N. A smaller t_G is consistent with a condensation-type transition

where macroscopic occupation of a quantum state occurs. This analysis together with the anomalous α implies that the $CaCrO_3$ crystal may actually undergo a BEC near 90 K.

The thermal conductivity κ reveals the dynamics of spins, lattice, and orbitals, which could give an important clue of what happens at T_N in $CaCrO_3$. Fig.3 shows the results of thermal conductivity measurements made on polycrystalline $CaCrO_3$ samples. It is impossible for us to measure the thermal conductivity on a 200 μm grain of $CaCrO_3$ crystal. However, measurements made on the sample C help to isolate a κ(T) that is essentially from the single crystal $CaCrO_3$; see SI[15] for detailed information. A small and weak temperature dependence of κ is found for both polycrystalline and single crystal $CaCrO_3$ samples over a broad temperature range above T_N. The κ(T) of $CaCrO_3$ is located between two extreme oxide cases, *i.e.* an amorphous oxide and a $LaGaO_3$ crystal. The $LaGaO_3$ crystal serves as an example of phonon thermal conductivity since it is a diamagnetic insulator. On the other hand, the minimum thermal conductivity κ_{min} can be calculated from an amorphous oxide in which the mean-free path is not longer than the interatomic distance. The κ of $CaCrO_3$ is close to a phonon thermal conductivity in magnitude near room temperature; but the temperature dependence is characteristic of an amorphous oxide. The thermal conductivity in a solid is described by $\kappa = \left(\frac{1}{3}\right) C\upsilon\ell$, where C is the specific heat, υ the acoustic sound velocity and ℓ the mean free path. In a glass, the temperature dependence of κ is dominated by the C since the ℓ for short-range phonons is small.[27] The κ of $CaCrO_3$ resembles the temperature dependence of C_p since ℓ is a constant in this amorphous-like oxide. The magnetic transition at T_N causes an abrupt drop of κ, which is clearly observed in sample C. However, the drop is diminished in the sample A and B as shown in the inset of Fig.3(a). An amorphous-like κ(T) has been seen in other crystalline oxides with an orbital degeneracy. However, a further reduction from the amorphous-like κ of $CaCrO_3$ on cooling through T_N is highly unusual.

Inverse κ versus temperature of several Mott insulators are plotted in Fig.3(b). Each of them offers different stories of how magnetic ordering and orbital ordering influence the thermal conductivity. $YCrO_3$ has no orbital degeneracy and exhibits type-G AF ordering at T_N. The κ(T) of $YCrO_3$ in the paramagnetic phase resembles that of $LaGaO_3$. The κ increases on cooling through T_N because of the magnon contribution and reduced scattering between spin excitations

and phonons in the magnetically ordered phase. YVO_3 has the same electronic configuration, *i.e.* $t_2^2e^0$ as that of $CaCrO_3$; however, the orbital degeneracy in YVO_3 survives only down to 180 K. Orbital fluctuations contribute a glassy κ for T > 180 K. At the orbital ordering transition T_{OO}, the κ bottoms out. A phonon-like κ is restored at $T < T_{OO}$ since a long periodicity in the lattice is established due to the orbital ordering. On cooling through $T_N < T_{OO}$, YVO_3 experiences a spin disorder-order transition where the κ is further enhanced. A phonon κ is finally realized through a first order transition at $T_{CG} < T_N$.[28] In $LaTiO_3$, the orbital degeneracy survives in the entire temperature range of the paramagnetic phase. On cooling through T_N, the spin/orbital ordering restores the phonon-like thermal conductivity.[29] These experiments clearly reveal how sensitive the thermal conductivity is as a probe for spin and orbital orderings and show a general trend that orbital ordering and spin ordering restore thermal conductivity. While a glassy κ in the paramagnetic phase of $CaCrO_3$ is clearly related to the orbital degeneracy, the sharp drop of κ on cooling through T_N distinguishes $CaCrO_3$ from any oxide systems studied so far. Critical fluctuations would cause a small dent around a magnetic transition temperature, *i.e.* a small drop and then a coming back of κ; see the data for CoF_2 for example.[30] But the influence of critical fluctuations on the thermal conductivity is fundamentally different from what happens at T_N in $CaCrO_3$. After exhausting all possible consequences of spin/orbital ordering, we focused on whether a BEC can account for the observed drop in κ on cooling through T_N.

As interacting Bose particles condense, it is acknowledged that condensed particles carry no entropy and make no contribution to the thermoelastic properties.[31] Condensed particles normally represent a very small fraction of all particles in a real system. As a result, the impact to the thermal conductivity from condensed particles is negligible compared to that from normal particles. In ^{4}He, a five-order jump of κ occurs on cooling through the λ point.[32] In all quantum spin systems, the magnetic state below T_N is not different from a classic Néel state.[23] A jump of κ due to the magnon contribution on cooling through T_N has always been found in these quantum spin systems.[33-36] On the other hand, in heavy metal superconductors like Pb, for example, electrons in states within a range of kT around the Fermi energy are dominant heat carriers. As these electrons form Cooper pairs and condense at $T < T_c$, the κ drops,[37] which demonstrates that condensed Bose particles carry no entropy.

In order to find possible particles/quasiparticles in $CaCrO_3$ that condense at T_N, we start from the local crystal structure since it reflects the electron and the orbital state. CrO_6 octahedra in $CaCrO_3$ are slightly compressed, *i.e.* c/a < 1, at room temperature.[5] This local site distortion is contrary to the intrinsic distortions in a *Pbnm* perovskite structure that would bias an orbital ordering leading to long, medium, and short Cr-O bonds.[13,14] A compressed CrO_6 octahedron is compatible with the orbital occupation of xy (l_z=0) and yz±izx ($l_z = \pm 1$) for a t_2^2 electron manifold. The spin-orbit coupling would make the spin easy axis along the *c* direction if the orbital angular momentum is not quenched. The observation of an easy magnetic axis along the *b* axis,[5] however, indicates that the orbital angular momentum is fully quenched. Moreover, an abrupt collapse of the Cr-O bond length along the *c* axis and an expansion in the *ab* plane on cooling through T_N in a type-C antiferromagnet are just opposite to what would be predicted for a localized-electron magnetostrictive distortion. We are, therefore, forced to conclude that, at least below T_N, there are itinerant yz, zx electron in a narrow *c*–axis π* band that is ¼-filled, which is consistent with ferromagnetic *c*-axis coupling of the localized xy spins that are antiferromagnetically coupled in the basal plane. Although the Cr-O bond lengths as well as the lattice parameters (excluding the volume) changes abruptly at T_N, the magnetic ordering and the c/a changes leave the transition second-order as indicated by the critical fluctuations seen in the specific-heat data. Since a classic orbital ordering is not an option here, we turn to the possibility that the xy orbital occupation undergo a BEC to account for the drop in the κ on cooling through T_N.

Whether particles can undergo a BEC depends critically on number conservation.[23] In a typical orbitally ordered phase, as is found in the paramagnetic phase of $LaMnO_3$ below750 K, the orbital excitations are described as orbitons.[38] The number of orbitons is not conserved. Analogous to quantum magnets where a BEC causes a sharp increase of magnetization, the Bose density in $CaCrO_3$ corresponds to the a/c ratio of an octahedron. The xy orbital occupation and/or localization leads to abrupt expansion of the *ab* plane and increase of a/c >1. Thermal vibrations involve all possible atomic displacements allowed by the crystal symmetry, which include modes associated with the orbital occupation. In quantum magnets,[33-36] heat flux carried by magnetic excitations is negligible in compared to that by lattice vibrations. A jump of κ at T_c may reflect the influence of a BEC to the lattice. In $CaCrO_3$, however, the lattice vibrations associated with

the xy orbital occupation no longer contribute to the κ at $T \leq T_N$. A slightly smaller C_p of the crystal sample than that of polycrystalline samples at $T < T_N$, see the inset of Fig.2(a), may indicate fewer degrees of freedom available for heat carriers. The analysis of thermal conductivity is highly consistent with a possible BEC from the critical behavior of C_p. The extremely sharp magnetic transition in single crystal $CaCrO_3$ may be interpreted on the basis of a BEC. As a matter of fact, the BEC model for $TlCuCl_3$ predicts an abrupt jump of magnetization on cooling through T_c.

In summary, oxygen-stoichiometric single-crystal $CaCrO_3$ exhibits three unprecedented features: (1) localized and itinerant electrons coexist in π-bonding t_2 orbitals on the same atom in the structure, (2) the bias effect by the intrinsic distortion in the *Pbnm* perovskite structure is entirely overwhelmed by the coexistence of itinerant yz, zx electrons and localized xy electrons, (3) a drop in thermal conductivity on cooling through T_N. We believe the experimental data manifest a BEC at T_N in $CaCrO_3$. A BEC of the orbital occupation accounting for (3) relies largely on the peculiar electron and orbital status in (1) and (2).

Acknowledgment

This work was supported by the National Science Foundation (DMR MIRT 1122603) and the Robert A Welch Foundation, Houston, Texas in the US. JAA, RMC, JSB, and MTF thank the Spanish MINECO project MAT2013-41099-R and RyC-2010-06276 for financial support. JSZ is grateful for the enlightening discussions with V. Zapf and S. Chernyshev.

*jszhou@mail.utexas.edu

References

1. B.L. Chamberland, Solid State Commun. **5**, 663 (1967)
2. J.B. Goodenough, J.M. Longo, and J.A. Kafalas, Mater. Res. Bull. **3**.471 (1968)
3. J.-S. Zhou, C.-Q. Jin, Y.-W. Long, L.-X. Yang, and J.B. Goodenough, Phys. Rev. Lett. **96**, 046408 (2006)
4. A.C. Komarek, et al Phys. Rev. Lett. **101**, 167204 (2008)
5. A.C. Komarek, et al Phys. Rev. B **84**, 125114 (2011)
6. S.V. Streltsov, M.A. Korotin, V.I. Anisimov, and D.I. Khomskii, Phys. Rev. B **78**, 054425 (2008)
7. P.A. Bhobe, et al, Phys. Rev. B **83**, 165132 (2011)

8. H.M. Liu, C. Zhu, C.Y. Ma, S. Dong, and J.-M. Liu, J. Appl. Phys. **110**, 073701 (2011)
9. J.F. Weiher, B.L. Chamberland, J.L. Gillson, J. Solid State Chem. 3, 529 (1971)
10. J. Zhao, N.L. Ross, D. Wang, and R.J. Angel, J. Phys. Conden. Matter **23**, 455401 (2011)
11. H. Falcon, J.A. Alonso, M.T. Casais, M.J. Martinez-Lope, and J. Sanchez-Benitez, J. Solid State Chem. **177**, 3099 (2004)
12. A.C. Komarek, H. Roth, M. Cwik, W.D. Stein, J. Baier, M. Kriener, F. Bouree, T. Lorenz, and M Braden, Phys. Rev. 75, 224402 (2007)
13. J.-S Zhou and J.B. Goodenough, Phys. Rev. Lett. 94, 65501 (2005)
14. J.-S Zhou and J.B. Goodenough, Phys. Rev.B 77, 132104 (2008)
15. Detailed information about sample's synthesis and characterization, structural refinement and parameters, measurement of the thermal conductivity, the analysis of specific heat.
16. E.F. Bertaut, Magnetism, III ed. G.T. Rado and H. Suhl, Academic Press (New York 1963)
17. T. Moriya, Phys. Rev. 120, 91 (1960)
18. J.-G. Cheng, J.-S. Zhou, J.B. Goodenough, H.D. Zhou, C.R. Wiebe, T. Takami, and T. Fujii, Phys. Rev. B 80, 134428 (2009)
19. L.J. de Jongh and A.R. Miedema, Adv. Phys. **23**, 1 (1974)
20. H.E. Stanley*, Introduction to phase transition and critical phenomena* (Oxford University Press, New York, 1971)
21. J. Wilks and D.S. Betts, *An Introduction to Liquid Helium*, (Oxford University Press, New York, 1987)
22. A.A. Aczel, et al. Phys. Rev. Lett. **103**, 207203 (2009)
23. V. Zapf , M. Jaime, and C.D. Batista, Rev. Mod. Phys. 86, 563 (2014)
24. T. Giamarchi, C. Ruegg, and O. Tchernyshyov, Nature Physics, 4, 198 (2008)
25. K.G. Wilson, Phys. Rev. B4, 3174 (1971)
26. C. Enss and S. Hunklinger, *Low-Temperature Physics*, p73, (Springer, Berlin 2005)
27. R. Berman, Thermal Conductivity in Solids, p104 (Oxford University Press, New York, 1976)
28. J.-Q. Yan, J.-S. Zhou, and J.B. Goodenough, Phys. Rev. Lett. **93**, 235901 (2004)
29. J.-G. Cheng, Y. Sui, J.-S. Zhou, J.B. Goodenough, W.H. Su, Phys. Rev Lett. 101, 87205 (2008)
30. H. Stern, J. Phys. Chem. Solids, 26, 153 (1965)
31. T.H.K. Barron and G.K. White, Heat Capacity and Thermal Expansion at Low Temperatures, p144, (Kluwer Academic, New York 1999)
32. F. Pobell, Matter and Methods at Low Temperatures, p23 (Springer Berlin 2007)
33. K. Kudo, M. Yamazaki, T. Kawamata, T. Noji, Y. Koike, T. Nishizaki, N. Kobayashi, H. Tanaka, J. Phys. Soc. Japan, 73, 2358 (2004)

34. Y. Kohama, A.V. Sologubenko, N.R. Dilley, V.S. Zapf, M. Jaime, J.A. Mydosh, A. Paduan-Filho, K.A. Al-hassanieh, P. Sengupta, S. Gangadharaiah, A.L. Chernyshev, and C.D. Batista, Phys. Rev. Lett. 106, 37203 (2011)
35. M. Sato, T. Kawamata, K. Naruse, K. Kudo, N. Kobayashi, Y. Koike, J. of Phys, Conf. Ser. 400, 32079 (2012)
36. X.F. Sun, W. Tao, X.M. Wang, and C. Fan, Phys. Rev. Lett. 102, 167202 (2009)
37. N.W. Ashcroft and N.D. Mermin, Solid State Physics, Brooks/Cole 1976
38. E. Saltoh, S. Okamoto, K.T. Takahashi, K. Tobe, K. Yamamoto, T. Klmura, S. Ishihara, S. Maekawa, Y. Tokura, Nature, 410, 180 (2001)

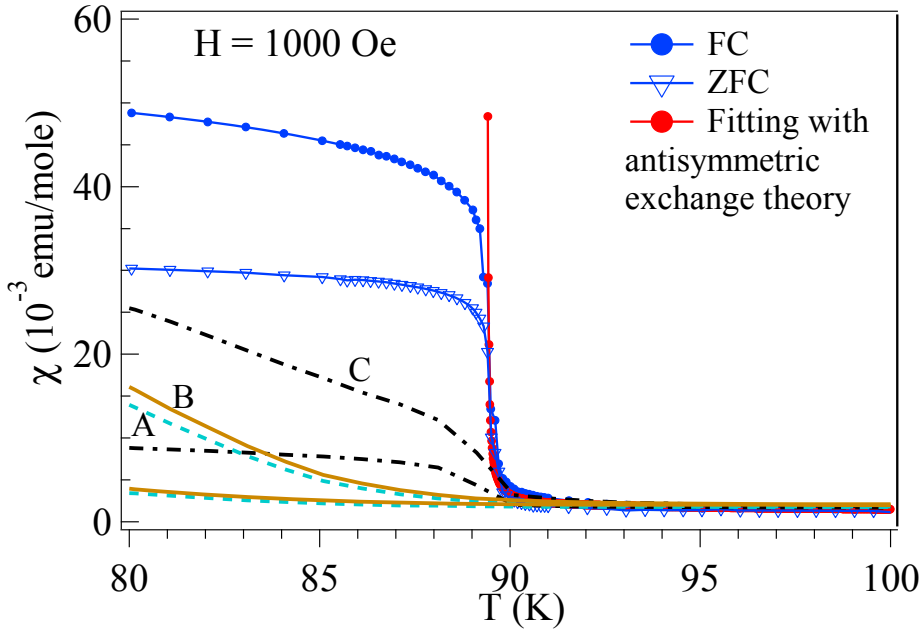

Fig.1 Temperature dependence of magnetization for (a) single crystal and (b) polycrystalline samples of $CaCrO_3$.

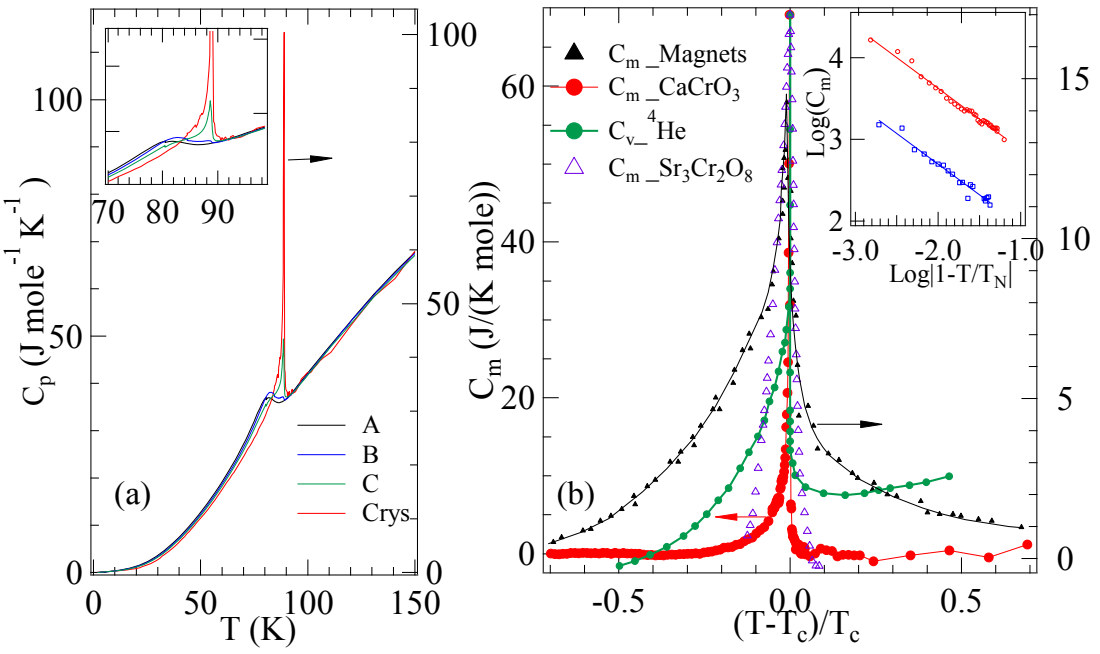

Fig.2 (a) Temperature dependence of specific heat for a variety of CaCrO3 samples; the inset: a zoom-in plot of the transition area; (b) the magnetic contribution C_m versus reduced temperature $(T-T_c)/T_c$ for $CaCrO_3$, Heisenberg magnets , and the λ transition in ^{4}He for comparison.

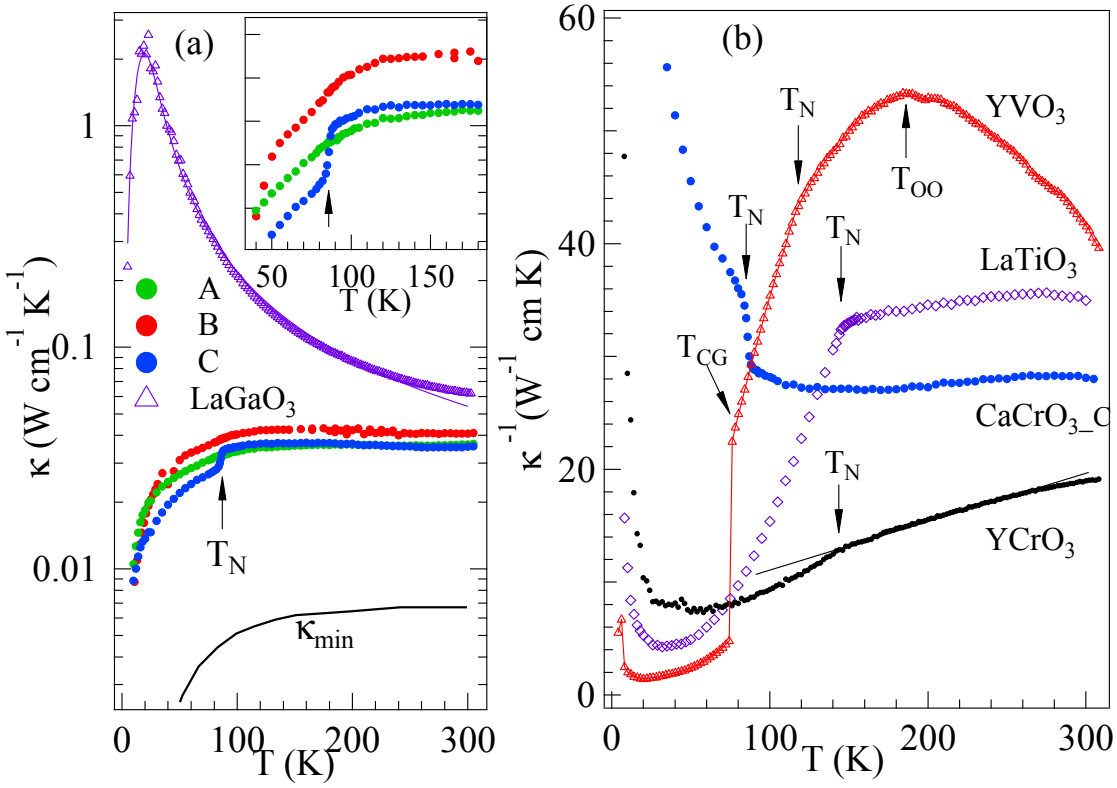

Fig.3. (a) Temperature dependence of thermal conductivity for a variety of $CaCrO_3$ samples and $LaGaO_3$ crysrtal; inset: a zoom-in plot of the transition area of the $CaCrO_3$ samples; a solid line inside the data of $LaGaO_3$ represents the fitting result to the Boltzmann formula; (b) the inverse thermal conductivity versus temperature for a $CaCrO_3$ sample and YVO_3, $YCrO_3$, and $LaTiO_3$ for comparison.